Lawrence Berkeley National Laboratory
Recent Work

Title
The active fracture model: Its relation to fractal flow patterns and a further evaluation using field observations

Permalink

Journal

Authors
Liu, Hui-Hai
Zhang, Guoxiang
Bodvarsson, Gudmundur S.

Publication Date
2003-05-30

The Active Fracture Model:

Its Relation to Fractal Flow Patterns and a Further Evaluation using Field Observations

Hui-Hai Liu, Guoxiang Zhang, and Gudmundur S. Bodvarsson

Earth Sciences Division
Lawrence Berkeley National Laboratory
Berkeley, California

ABSTRACT

The active fracture model (AFM) (Liu et al., 1998) has been widely used in modeling flow and transport in the unsaturated zone of Yucca Mountain, Nevada, a proposed repository of high-level nuclear wastes. This study presents an in-depth evaluation of the AFM, based on both theoretical arguments and field observations. We first argue that flow patterns observed from different unsaturated systems (including the unsaturated zone of Yucca Mountain) may be fractals. We derive an interesting relation between the AFM and the fractal flow behavior, indicating that the AFM essentially captures this important flow behavior at a subgrid scale. Finally, the validity of the AFM is demonstrated by the favorable comparison between simulation results based on the AFM and C-14 age and fracture coating data collected from the unsaturated zone at Yucca Mountain. These data sets independently provide important insight into flow and transport processes at the Yucca Mountain site. Potential future improvements of the AFM include expanding it to consider film flow and multifractal concepts.

1   Flow and transport in unsaturated fractured rocks are generally complicated because

2   of the complexity of fracture-matrix interaction mechanisms, distinct differences in

3   hydraulic properties between fractures and the matrix, and nonlinearity involved in

4   unsaturated flow. Recently, the investigation into using the unsaturated zone at Yucca

5   Mountain, Nevada, as a storage facility for the geological disposal of high-level nuclear

6   wastes has generated intensive research interests in modeling flow and transport in

7   unsaturated fractured rocks (e.g., Bodvarsson and Tsang, 1999; Robinson et al. 1997;

8   Pruess et al., 1999; Liu et al. 1998; Ho, 1997). To reliably assess the performance of the

9   repository, it is desirable to accurately predict flow and transport processes within the

10   mountain. Modeling flow and transport in unsaturated fractured rocks is also of interest in

11   other areas including environmental contamination in arid and semiarid regions.

12   Several approaches are available in the literature for modeling flow and transport in

13   unsaturated fractured rocks. When classified according to the manner in which fracture

14   networks are treated in the model structure, these approaches mainly fall into one of the

15   two categories: the continuum approach and the discrete fracture network approach.

16   Excellent reviews on these approaches, which have been developed and used in different

17   fields (including oil reservoir engineering, groundwater hydrology, geothermal

18   engineering and soil physics), can be found in Bear et al. (1993), National Research

19   Council (1996) and Pruess et al. (1999).

20   In the continuum approach, fractures are considered to be sufficiently ubiquitous and

21   distributed in such a manner that they can be meaningfully described statistically (Bear et

22   al., 1993). The role of individual fractures in fractured media is considered to be similar

23   to that of individual pores in porous media. Therefore, one can describe average fracture

properties as macroscopic and those associated with individual fractures as microscopic. In the continuum approach, connected fractures and rock matrix are viewed as two or more overlapped interacting continua. In other words, at a "point," two or more continua are considered to co-exist. In this case, the continuum mechanics formulations, such as those used for porous media, can be used to describe flow and transport in each continuum. Coupling of processes between different continua is determined by their interaction mechanisms at a subgrid scale.

The fracture network approach involves the generation, by computer simulation, of synthetic fracture networks, and the subsequent modeling of flow and transport in these networks. The approach has been extensively used for single-phase flow and transport, with deterministic, stochastic, artificial, or site-specific fracture networks (e.g., Bear et al. 1993; National Research Council, 1996), and has recently been applied to unsaturated conditions (Rasmussen, 1991; Kwicklis and Healey, 1993; Karasaki et al. 1994; Zimmerman and Bodvarsson, 1996; Liu and Bodvarsson, 2001; Liu et al., 2003a).

Both continuum and fracture network approaches have advantages and disadvantages. While the fracture network approach is useful as a tool for concept evaluation or model-based process studies, it has several limitations. First, the approach requires geometric parameters that may strongly impact flow and transport, such as fracture apertures and conductivity, but typically cannot be well constrained from field observations (Pruess et al., 1999). Second, it is difficult to separate the conductive fracture geometry from the non-conductive fracture geometry (National Research Council, 1996). Third, flow and transport models based on the approach can be complex and computationally intensive for realistic fracture densities (National Research Council, 1996). Fourth, so far, the

studies based on the fracture network approach have rarely considered fracture-matrix interaction (flow and transport between fractures and the matrix), because of computational intensity for unsaturated flow and transport (Pruess et al., 1999). The fracture-matrix interaction has important effects on flow and transport processes in unsaturated fractured rocks. Because the continuum approach is relatively simple and straightforward to implement, it is preferred for most applications encountered in practice (National Research Council, 1996). For example, because the number of fractures is on the order of 10^9 at Yucca Mountain (Doughty, 1999), it is practically impossible to construct and calibrate a discrete fracture network site-scale model with so many fractures, considering data availability and computational feasibility. Therefore, the dual-continuum approach, in which fractures and the matrix are treated as two overlapping and interactive continua, has been used as the baseline approach for modeling flow and transport within Yucca Mountain (Bodvarsson and Tsang, 1999; Liu, 2000). Note that a similar approach has also been used to model unsaturated flow and transport in structured soils (Gerke and van Genuchten, 1993).

A traditional continuum approach assumes uniformly distributed flow patterns at a subgrid scale and therefore cannot be used for representing gravity-driven fingering flow and transport in fracture networks, resulting from subsurface heterogeneities and nonlinearity involved in unsaturated flow (Glass, 1996; Liu et al., 1998; Sue et al., 1999; Pruess et al., 1999). In an effort to incorporate this flow behavior into the continuum approach, Liu et al. (1998) developed an active fracture model (AFM) that assumes only a portion of fractures in a connected unsaturated fracture network to contribute to liquid water flow. Because the AFM can provide a large range of flow behaviors in unsaturated

fractures (including fast flow behavior), it has been used extensively for modeling large-scale flow and transport in the unsaturated zone of Yucca Mountain (e.g., Moridis and Hu, 2000; Wu et al., 2000; Wu et al., 2002; Liu et al., 2003b; Zhou et al., 2003; Buscheck et al., 2002; Xu et al., 2003).

While previous studies have shown that simulation results based on the AFM are generally consistent with field observations from the unsaturated zone of Yucca Mountain (Liu et al., 1998; Liu et al., 2003b), a more in-depth evaluation of the AFM is highly desirable, because accurately modeling complex, large-scale flow and transport within unsaturated fractured rocks is of interest to many research areas. Therefore, the major objective of this work is to provide a further evaluation of the AFM, based on both theoretical arguments and field observations. In this paper, we first show that flow patterns in unsaturated systems (including the unsaturated zone of Yucca Mountain) may be characterized by fractals. Then we will show that the AFM is approximately consistent with fractal flow patterns at the subgrid scale. Finally, we demonstrate that simulation results based on the AFM can represent different data sets collected from the Yucca Mountain site. These data sets contain important information about large-scale flow and transport processes at the site.

ACTIVE FRACTURE MODEL

The AFM was developed within the context of the dual-continuum approach (Liu et al., 1998). While the details of the AFM can be found in Liu et al. (1998), a brief introduction of the AFM is provided here for convenience. The active fracture concept is based on the reasoning that, because of the fingering flow, only a portion of fractures in a

connected, unsaturated fracture network contribute to liquid water flow, while other fractures are simply bypassed. The portion of the connected fractures that actively conduct water are called active fractures. We hypothesize that the number of active fractures in the unsaturated zone of Yucca Mountain is small compared to the total number of connected fractures such that active fractures, rather than total connected fractures, must be used in numerical models. We further hypothesize that the number of active fractures within a gridblock is large; hence, the continuum approach is still valid for describing fracture flow. These hypotheses are consistent with the consideration that fractures conducting water in the unsaturated zone of Yucca Mountain are many and highly dispersed (Liu, 2000).

To use the active fracture concept for modeling flow and transport in fractures, we treat active fractures as a portion of the "homogeneous" fracture continuum for a given gridblock. Note the differences between the active fracture model and the conventional, capillary-equilibrium-based, fracture-water distribution model. The latter assumes that liquid water occupies first fractures with small apertures, and then fractures with relatively large apertures, as water potential (or water saturation) increases. In contrast, the active fracture model presumes gravity-dominated, nonequilibrium, preferential liquid water flow in fractures, which is expected to be similar to fingering flow in unsaturated porous media. A liquid finger can bypass a large portion of a porous medium, which does not necessarily correspond to large pores. Note that the above discussion is valid for large-scale flow processes and not inconsistent with possible validity of a capillary-equilibrium-based water distribution concept at relatively small scales corresponding to an individual flow path or a single flow finger.

1   Flow and transport conditions and fractured rock properties should determine the

2   fraction of active fractures in a connected fracture network, f_a. An expression for f_a must

3   satisfy the following conditions: all connected fractures are active ($f_a = 1$) if the system is

4   fully liquid saturated; all fractures are inactive ($f_a = 0$) if the system is at residual

5   saturation; and f_a should be related to water flux in fractures. It is generally believed that

6   more fractures are conducive to a larger water flux. This water flux in fractures is

7   considered to be mainly dependent on fracture saturation because fracture water flow is

8   gravity-dominated. A simple expression for f_a (-), which meets these conditions and

9   includes only one parameter, is a power function of effective water saturation in

10   connected fractures, S_e (-):

11
$$f_a = S_e^{\gamma}$$
[1]

12

13   where γ (-) is a positive constant depending on properties of the corresponding fracture

14   network, and the effective water saturation in connected fractures is given by

15
$$S_e = \frac{S_f - S_r}{1 - S_r}$$
[2]

16

17   where S_f (-) is the water saturation of all connected fractures and S_r is the residual fracture

18   saturation. In this study, Eq. [1] is used to determine the fraction of active fractures. As

19   will be discussed below, this simple equation is actually the first-order approximation for

20   fractal flow behavior at a subgrid scale, although it was initially developed as an

21   empirical relation (Liu et al., 1998).

1   Note that only the active fracture continuum, a portion of the total fracture continuum,

2   contributes to flow and transport in fractures and fracture-matrix interaction. Fracture

3   hydraulic properties should thus be defined for active fractures. The effective water

4   saturation of active fractures, S_{ae} (-), is related to the effective water saturation in

5   connected fractures, S_e, by

6
$$S_{ae} = \frac{S_e}{f_a} = S_e^{\,1-\gamma}$$
[3]

7

8   Because $S_{ae} \leq 1$, γ should be smaller than or equal to one. The effective water saturation

9   of active fractures is related to the actual water saturation in active fractures, S_a, by

10
$$S_{ae} = \frac{S_a - S_r}{1 - S_r}$$
[4]

11

12   If all connected fractures are considered to be active in conducting water, as assumed in

13   previous studies, the water capillary pressure for the fracture continuum may be

14   described by the well-known van Genuchten relation (van Genuchten 1980):

15
$$P_c(S_e) = \frac{1}{\alpha}[S_e^{\,-1/m} - 1]^{1/n}$$
[5]

16

17   where α, (Pa^{-1}), n, (-) and $m=1-1/n$ are van Genuchten parameters. In the active fracture

18   model, however, the van Genuchten capillary-pressure relation is considered to be

19   relevant for the active fracture continuum, rather than for the whole fracture continuum.

9

The capillary pressure for active fractures is determined by replacing S_e in Eq. [5] with S_{ae}:

$$P_c(S_e) = \frac{1}{\alpha}[S_{ae}^{-1/m} - 1]^{1/n} = \frac{1}{\alpha}[S_e^{(\gamma-1)/m} - 1]^{1/n} \qquad [6]$$

Eq. [6] rather than [5] should be used to simulate water flow in the fracture continuum. For a given effective water saturation in connected fractures, a larger γ value corresponds to a larger effective water saturation in active fractures, and therefore to a lower absolute value for capillary pressure.

The liquid-phase relative permeability for the active fracture continuum, k_{ar} (-), is directly determined by the effective water saturation of active fractures. However, because only a portion of the fractures are active, the relative permeability of the entire fracture continuum, k_r, (-) should be the relative permeability of active fractures multiplied by f_a, or

$$k_r = f_a k_{ar} = S_e^{\gamma} k_{ar} \qquad [7]$$

where k_{ar} can be given by the following van Genuchten permeability relation:

$$k_{ar} = S_{ae}^{1/2}[1 - \{1 - S_{ae}^{1/m}\}^m]^2 = S_e^{(1-\gamma)/2}[1 - \{1 - S_e^{(1-\gamma)/m}\}^m]^2 \qquad [8]$$

Combining Eqs. [7] and [8] yields

$$k_r = S_e^{(1+\gamma)/2}[1 - \{1 - S_e^{(1-\gamma)/m}\}^m]^2 \qquad [9]$$

1   In general, relative permeability (k_r) is affected by γ in a complicated manner for a given

2   S_e. A larger γ value, resulting in a higher effective water saturation in active fractures

3   (S_{ae}), gives rise to a larger value of k_{ar}. On the other hand, a larger γ value corresponds to

4   a smaller value of f_a. Because the former effect is dominant, a larger γ value gives a

5   larger relative permeability for a given effective water saturation of the fracture

6   continuum.

7   Note that the van Genuchten relationships were developed for porous media rather

8   than fracture networks. Recently, Liu and Bodvarsson (2001) developed a new

9   constitutive-relationship model for unsaturated flow in fracture networks, based mainly

10   on numerical experiments. They found that the van Genuchten model is approximately

11   valid for low fracture saturations corresponding to the ambient conditions in the

12   unsaturated zone of Yucca Mountain. Therefore, the van Genuchten relationships are

13   still employed because it is the ambient flow process that is of interest here. However, we

14   emphasize that the key hypothesis of the AFM is Eq. [1]. This equation can be combined

15   with any appropriate constitutive-relationship model to simulate unsaturated flow

16   processes in fractured porous media. Consequently, the focus of this work is on

17   evaluation of Eq. [1].

18   In an unsaturated fracture network, the ratio of the interface area contributing to

19   flow and transport between fractures and the matrix, to the total interface area determined

20   geometrically from the fracture network, is called the fracture-matrix interface area

21   reduction factor. In the active fracture model, this reduction factor results from three

22   considerations. First, the average interface area between mobile water in an active

1   fracture and the surrounding matrix is smaller than the geometric interface area. Second,

2   the number of active fractures is smaller than that of connected fractures. (Conventionally,

3   all connected fractures are assumed to contribute to fracture-matrix interaction). Third,

4   average active fracture spacing is much larger than that for connected fractures. Under

5   the quasi-steady-state condition, flow and transport between fractures and surrounding

6   matrix is inversely proportional to the corresponding fracture spacing. Based on these

7   considerations, Liu et al. (1998) derived an expression for the reduction factor:

8
$$R \cong S_e^{1+\gamma}$$
[10]

9

10   In summary, the active fracture model uses a combination of the volume-averaged

11   method and a simple filter to deal with fracture flow and transport. Inactive fractures are

12   filtered out in modeling fracture-matrix interaction, flow, and transport in the fracture

13   continuum. The γ factor may be interpreted as a measure of the "activity" of connected

14   fractures. Generally speaking, a smaller γ value corresponds to a larger number of active

15   fractures in a connected fracture network. For example, $\gamma = 0$ results in $f_a = 1$ in Eq. [1],

16   corresponding to all connected fractures being active. On the other hand, $\gamma = 1$

17   corresponds to zero fracture capillary pressure (Eq. [6]), indicating that all active

18   fractures are saturated. In the latter case, the fraction of active fractures is very small for

19   small percolation fluxes, because relatively high fracture permeabilities allow most of the

20   water to flow through only a few fractures.

21

22

1   **THE AFM AND FRACTAL FLOW BEHAVIOR IN UNSATURATED SYSTEMS**

2   A flow system exhibits so-called fractal flow behavior when the corresponding flow

3   patterns can be characterized by fractals. In this section, a brief discussion of fractal

4   dimension (used for characterizing fractal patterns) is presented, followed by a discussion

5   of evidence for fractal flow behavior in unsaturated systems and relations between the

6   AFM and this fractal flow behavior.

7   **Fractal Dimension**

8   Fractal dimension, d_f, is generally a noninteger and less than the corresponding

9   Euclidean (topological) dimension of a space, D. Different kinds of definitions of fractal

10   dimension exist (e.g., similarity dimension, Hausdorff dimension, and box dimension),

11   although they provide very close fractal dimension values for practical applications

12   (Feder, 1988). The most straightforward definition is the so-called box dimension, based

13   on a simple "box-counting" procedure. This dimension is determined from Eq. [11]

14   (below) by counting the number (N) of "boxes" (e.g., line segment, square and cubic for

15   one-, two-, and three-dimensional problems, respectively), needed to cover a spatial

16   pattern, as a function of the box size (l) (e.g., Feder, 1988):

17

18    $$N(l) = \left(\frac{L}{l}\right)^{d_f}$$ [11]

19

20   where L refers to the size of the entire spatial domain under consideration. Figure 1

21   shows a box-counting procedure for a spatial pattern with $d_f = 1.6$, in a two-dimensional

1   domain with size L (Yamamoto et al., 1993).

2

3   Obviously, if a spatial pattern is uniformly distributed in space, the fractal dimension

4   will be identical to the corresponding Euclidean dimension. In this case, the box number,

5   N*, and the box size l have the following relation

6

7    $$N*(l) = \left(\frac{L}{l}\right)^D \qquad\qquad\qquad [12]$$

8   A fractal pattern exhibits similarity at different scales. When $d_f < D$, the corresponding

9   pattern does not fill the whole space, but only part of it (Fig. 1).

10   **Fractal Flow Behavior in Unsaturated Systems**

11   Fractals have been shown to provide a common language for describing many

12   different natural and social phenomena (Mandelbrot, 1982). While a vast literature exists

13   on the validity of the fractal concept for a great number of fields, fractals have been

14   found to be useful for representing many spatial distributions in subsurface hydrology,

15   including soil particle size distribution, roughness of fracture surface, distribution of

16   permeability in heterogeneous formations, and large-scale solute dispersion processes

17   (e.g., Tyler and Wheatcraft, 1990; Rieu and Sposito, 1991a, b; Perfect et al., 1996;

18   Neuman, 1990, 1994; Molz and Boman, 1993; Molz et al., 1997). Especially, recent

19   studies have suggested that complex flow (or solute transport) patterns in unsaturated

20   systems can be characterized by fractals (below).

21

22   Flury and Flühler (1995) first indicated that solute leaching patterns, observed from

23   three field plots consisting of an unsaturated loamy soil, could be well represented by a

diffusion-limited aggregation (DLA) model (Witten and Sander, 1981), although the

relation between DLA parameters and soil hydraulic properties is still an unresolved issue.

It has been documented that DLA generates fractal patterns (e.g., Feder, 1988; Flury and

Flühler, 1995). The observation of Flury and Flühler (1995) is further supported by a

study of Persson et al. (2001), who used dye-infiltration data to investigate field pathways

of water and solutes under unsaturated conditions. Persson et al. (2001) showed that field

observations are well described by the DLA model. Furthermore, they demonstrated that

observed mean power spectrum for dye penetration of a field plot displays a typical

power-law relationship, another important indication of fractal flow behavior. Glass

(1993) first showed that unsaturated flow in a single vertical fracture is characterized by

gravity-driven fingers, and the resulting flow patterns could be modeled by an invasion-

percolation approach (Wilkinson and Wilemsen, 1983). Again, percolation-based models

generate fractal clustering patterns (Stauffer and Aharony, 2001). Closely related to flow

and transport processes in unsaturated systems, flow patterns observed from multiphase

systems are also related to fractals. For example, viscous fingering in porous media has

been experimentally shown to be fractal (Feder, 1988). The problem of viscous fingering

in porous media is of central importance in oil recovery. Smith and Zhang (2001) also

reported that DNAPL fingering in water saturated porous media, observed from sandbox

experiments, is fractal.

Detailed experimental studies on unsaturated flow patterns in large-scale fracture

networks are scarce in the literature, because of the technical difficulties in observing

these patterns in the field. Fortunately, some geochemical data sets closely related to flow

1   patterns in large-scale fracture networks have recently become available from the

2   unsaturated zone of Yucca Mountain. For example, a spatial distribution of fractures with

3   mineral coatings was determined along an underground tunnel, using a detailed-line-

4   survey method (Paces et al., 1996; Fabryka-Martin et al. 2000). The total survey length

5   along the tunnel is several thousand meters, broken up by a number of disconnected 30 m

6   survey intervals. As will be discussed below, fracture coating is roughly a signature of

7   water flow paths. Therefore, this data set can be used to infer potential fractal flow

8   behavior at a large fracture-network scale.

9

10   While the detailed line survey was performed for several geological units, we focus on

11   the one that is densely fractured (average fracture spacing is about 0.2 m) and has the

12   largest number of 30 m survey intervals. In this unit, about 130 coated fractures were

13   found over the approximate 1,000 m survey length. The intersections of coated fractures

14   with the survey line (along the underground tunnel) form a set of points. If the

15   corresponding flow pattern is fractal, the point set should be fractal too. A box-counting

16   method is used to detect the fractal pattern from this point set. Fig. 2 shows number of

17   boxes (line segments), N, covering at least one intersection point as a function of box size

18   (length of a segment), l. Note that the largest box size corresponds to the length of survey

19   intervals (30 m). The smallest box size used here is 3 m. If all fractures are coated, all

20   boxes of this size or larger should at least cover one of the intersection points, because

21   the average fracture spacing is much smaller than this size. This corresponds to a

22   dimension of one (the topological dimension) based on Eq. [11].

23

1

Fig. 2 shows that the data points can be fitted by a power function with a power of −0.5,

indicating the existence of a fractal pattern for coated fractures (or flow paths). The

power value suggests a fractal dimension of 0.5 that is not an integer but smaller than the

corresponding topological dimension (one). To the best of our knowledge, the fractal

flow behavior in large-scale unsaturated fracture networks, observed from field data, has

not been previously reported in the literature. While more studies may be needed to

further confirm the finding reported here, it is generally reasonable to expect the

existence of fractal flow behavior in large-scale unsaturated fracture networks, given the

evidence shown here and the fact that complex unsaturated flow patterns in several

different natural systems are fractals (and fractals are valid for describing many different

processes).

A Relation between the AFM and Fractal Flow Patterns

We have shown that flow processes in unsaturated systems (including fracture networks)

may be fractal. This has many important implications regarding the development of

numerical models for large-scale unsaturated systems, because fractal patterns are

generally related to fingering and/or preferential flow paths. In this section, we will

demonstrate the AFM's consistency with fractal flow behavior in unsaturated fracture

networks.

Consider Fig. 1(a) to be a gridblock containing a fracture network and the

corresponding flow pattern in the fracture network to be fractal. In this case, only a

portion of the medium within a gridblock contributes to water flow (Fig. 1). This is

conceptually consistent with the AFM (Liu et al. 1998). Note that in Fig. 1, a box is

shadowed if it covers one or more fractures (or fracture segments) that conduct water. For

simplicity, further consider that fractures are randomly distributed in space, and thus the

dimension for water-saturation distribution is the corresponding Euclidean dimension

when all the connected fractures actively conduct water. As will be obvious from the

derivations to follow, this assumption does not alter our general conclusion regarding the

connection between the AFM and fractal flow patterns.

Combining Eqs. [11] and [12] yields

$$[N(l)]^{1/d_f} = [N*(l)]^{1/D} \qquad\qquad\qquad [13]$$

The average water saturation (S_e) for the whole gridblock (Fig. 1(a)) is determined to be

$$S_e = \frac{V}{l^D \phi N*(l)} \qquad\qquad\qquad [14]$$

where V is the total water volume (excluding residual water) in fractures within the

gridblock (Fig. 1a), and ϕ is fracture porosity. Similarly, the average water saturation (S_b)

for shadowed boxes with a size of l is

$$S_b = \frac{V}{l^D \phi N(l)} \qquad\qquad\qquad [15]$$

1   From Fig. 1, it is obvious that there exists a box size $l_1 < L$ satisfying:

2    $$\frac{V}{l_1{}^D \phi} = 1$$ [16]

3   Based on Eqs. [13]–[16], the average saturation for shadowed boxes with size l_1, S_{b1}, can

4   be expressed by

5

6    $$S_{b1} = (S_e)^{\frac{d_f}{D}}$$ [17]

7   Because a fractal is similar at different scales, the procedure to derive Eq. [17] from

8   a gridblock with size L can be applied to shadowed boxes with the smaller size of l_1. In

9   this case, for a given box size smaller than l_1, the number of shadowed boxes will be

10   counted as an average number for those within the (previously shadowed) boxes with a

11   size of l_1. Again, we can find a box size $l_2 < l_1$ to obtain a saturation relation:

12   $$S_{b2} = (S_{b1})^{\frac{d_f}{D}} = (S_e)^{\left(\frac{d_f}{D}\right)^2}$$ [18]

13

14   The procedure to obtain Eq. [18] can be continued until it reaches an iteration level, n*,

15   at which all the shadowed boxes with a size of l_n cover active fractures only. The

16   resultant average saturation for these shadowed boxes is

17   $$S_{bn} = (S_e)^{\left(\frac{d_f}{D}\right)^{n*}}$$ [19]

18   By definition of active fractures, S_{bn} should be equivalent to the effective saturation

19   of active fractures. It is remarkable that Eq. [19] is similar to Eq. [3], obtained from a key

20   hypothesis of the AFM that the fraction of active fractures in an unsaturated fracture

network is a power function of the average effective saturation of the network. Comparing these two equations yields:

$$\gamma = 1 - \left(\frac{d_f}{D}\right)^{n*}$$ [20]

Eq. [20] provides the first theoretical relation between the AFM parameter γ and the fractal dimension, while γ was initially developed as an empirical parameter (Liu et al., 1998). Thus, the AFM essentially captures fractal flow behavior at the gridblock scale (d_f < D), whereas traditional continuum approaches assume a uniform flow pattern (or effective-saturation distribution) at that scale (corresponding to d_f = D or γ = 0). In other words, the AFM can be used for simulating fractal flow behavior (in an unsaturated fracture network) that cannot be handled by traditional continuum approaches.

A Preliminary Assessment of Saturation Dependency of the AFM Parameter γ

Eq. [20] implies that the AFM parameter γ is not a constant, as assumed by Liu et al. (1998), but a function of saturation (or other flow conditions), because both iteration level $n*$ and d_f may be dependent on water saturation for a given fracture network. The relations among $n*$, d_f, and the relevant flow conditions (such as saturation) are not totally clear at this point. However, a constant γ is a reasonable treatment at least for a limited range of water saturations (or flow conditions), which is the case for the unsaturated zone of Yucca Mountain where the fracture saturation is believed to be typically less than 10% under ambient conditions. On the other hand, experimental

1   evidence seems to indicate that γ is a weak function of saturation at least for porous

2   media under certain conditions (which will be discussed below). It is obvious from the

3   derivation of Eq. [20] that the AFM concept and Eq. [20] can be applied to porous media

4   also, as long as fingering flow patterns in them are fractals. With this in mind, results

5   from porous media may be used to conceptually evaluate the relation between γ and

6   water saturation for unsaturated fracture networks.

7

8   Based on laboratory experimental observations reported in the literature, Wang et al.

9   (1998) derived a relation between flow conditions and a parameter, F, defined as the ratio

10 of horizontal cross-sectional area occupied by gravity fingers, to the total cross-sectional

11 area. F corresponds to f_a that is defined as the portion of active fractures in a fracture

12 network (Eq.[1]). Wang et al. (1998) related F to the ratio of average water flux through

13 the whole cross-sectional area, q, to the saturated hydraulic conductivity of the porous

14 medium, K_s, as follows:

15 $$F \approx \left(\frac{q}{K_s} \right)^{1/2} \qquad\qquad [21]$$

16 for $q/K_s = 0.4 - 1.0$. By definition, we can relate the average water flux within fingers

17 (q_F) to q by

18 $$q_F = \frac{q}{F} \qquad\qquad [22]$$

19 and also relate the average water saturation of fingers, S_F, to the average water saturation

20 for the whole cross-sectional area, S_e, by

21 $$S_F = \frac{S_e}{F} \qquad\qquad [23]$$

1   It is expected that flow within a gravitational finger is gravity dominated. In this case, we

2   can approximately have

3    $$\frac{q_F}{K_s} \approx k_r = S_F{}^{\beta} \qquad\qquad [24]$$

4   Eq. [24] uses the Brooks-Corey (1964) model for describing relationship between relative

5   permeability (k_r) and saturation relationship, with β a constant. Combining Eqs. [21] to

6   [24] yields

7    $$F \approx (S_e)^{\frac{\beta}{1+\beta}} \qquad\qquad [25]$$

8   Comparing the above equation with Eq. [1] gives

9

10    $$\gamma \approx \frac{\beta}{1+\beta} \qquad\qquad [26]$$

11   Therefore, γ is a constant under certain conditions for porous media. Consequently, we

12   expect that γ may be a weak function of saturation for unsaturated fracture networks if

13   fingering flow patterns in a porous medium are considered to be analogous to flow

14   patterns in the networks. However, we acknowledge that this connection needs more

15   investigation in future studies.

16

17   **EVALUATION OF THE AFM USING FIELD OBSERVATIONS**

18

19   So far, we have shown that fractal flow behavior may be common in different

20   unsaturated systems (including unsaturated fracture networks) and also that the AFM is,

21   in general, consistent with this behavior. In this section, we will further evaluate the AFM

1   using different data sets collected from the Yucca Mountain site. Considering the

2   complexity of large-scale unsaturated flow and transport in fractured porous media, the

3   direct use of actual field data for evaluating a model is critical. Previously, it has been

4   shown that simulation results based on the AFM match the matrix saturation and water

5   potential data collected from long boreholes at the Yucca Mountain site (e.g., Liu et al.,

6   1998). These results are also consistent with flow and tracer transport data observed from

7   a field test (on a scale of about 20 m) performed in a densely fractured unit within Yucca

8   Mountain (Liu et al., 2003b). In this study, we focus on evaluating the AFM with C-14

9   age data and fracture coating data that provide important information regarding large-

10   scale unsaturated flow processes in fractures and fracture-matrix interaction.

11

12   **Geological Setting**

13   Geological formations of the unsaturated zone of Yucca Mountain have been

14   grouped into stratigraphic units (on the basis of welding) by Montazer and Wilson (1984).

15   The stratigraphic units consist of the following, in descending order from the land surface:

16   welded Tiva Canyon Tuff (TCw); mainly nonwelded Paintbrush Group (PTn); welded

17   Topopah Spring Tuff (TSw); mostly nonwelded and sometimes altered Calico Hills

18   Formation (CHn); and the mostly nonwelded and altered Crater Flat (undifferentiated)

19   Group (CFu). The nonwelded zones near the water table in the CHn and CFu can be

20   subject to zeolitic alteration that reduces the matrix permeability by orders of magnitude

21   (Bandurraga and Bodvarsson, 1999). Furthermore, 35 hydrogeologic layers are defined to

22   correspond to geologic formations and coincident hydrogeologic unit boundaries.

Welded formations are highly fractured, and nonwelded formations have relatively small fracture densities. Liquid water flow occurs mainly in the tuff matrix for nonwelded formations and in fractures for welded formations. Conceptual models of flow and transport in the unsaturated zone of Yucca Mountain can be found in Bodvarsson et al. (2001), Flint et al. (2001), and Liu (2000). For each of the 35 hydrogeologic layers, hydraulic properties include permeability and van Genuchten parameters for both fracture and matrix continua, with AFM parameter γ as an additional parameter. These properties are estimated by model calibration, based on small-scale property measurements, matrix saturation and potential data, and pneumatic data. The methodology of the model calibration has been reported in Bandurraga and Bodvarsson (1999), Liu et al. (1998) and Zhou et al. (2003).

C-14 Data

Carbon-14 data have been collected from perched water, pore water, and gas samples from the unsaturated zone of Yucca Mountain (Yang, 2002; Fabryka-Martin et al. 2000). Water travel times from ground surface to perched-water bodies were dominated by PTn, where flow occurs mainly in the rock matrix, and thus simulated water travel time to the groundwater table is insensitive to the AFM parameters. As a result, carbon-14 data collected from perched water are not used for validating the AFM. Pore-water carbon-14 data from various boreholes at Yucca Mountain may not be representative of the pore-water residence time because of probable contamination by atmospheric $^{14}CO_2$ during drilling, resulting in apparently younger residence times (Yang, 2002; Fabryka-Martin et

1   al. 2000). Carbon-14 data from gas samples are considered to be most representative of *in*

2   *situ* conditions (Yang, 2002). Atmospheric $^{14}CO_2$ during drilling is not expected to

3   contaminate those gas samples collected several years after drilling. Gas samples were

4   collected from two kinds of boreholes: open surface-based boreholes and instrumented

5   (closed) surface-based boreholes. Because the data from the latter boreholes (USW SD-

6   12 and USW UZ-1) are the most reliable indicators of *in situ* conditions (Fabryka-Martin

7   et al. 2000), carbon-14 residence ages (Fabryka-Martin et al. 2000) calculated using the

8   data from these two boreholes are used for validating the AFM.

9

10   Gas-phase carbon-14 ages are assumed to be representative of ages of the *in situ* pore

11   water. The rationale for this assumption is provided in detail by Yang (2002). This

12   assumption presumes rapid exchange of gas-phase CO_2 (in hours to days) with dissolved

13   CO_2 and (HCO_3^-) in pore water. Furthermore, the amount of C in an aqueous-phase

14   reservoir relative to C in the CO_2 gas-phase reservoir is a hundred times greater.

15   Consequently, the aqueous phase will dominate the gaseous phase when exchange

16   occurs, indicating the reasonableness of the assumption (Yang 2002).

17

18   **Fracture Coating Data**

19   The process of unsaturated-zone mineral deposition is initiated during infiltration

20   where meteoric water interacts with materials in the soil, after which a portion may then

21   enter the bedrock fracture network. Fracture coating is generally a signature of water flow

22   paths. Thus, the coating data are useful for validating the AFM that describes water flow

23   in fractures.

1

2   Fracture coating data were collected in an underground tunnel in the unsaturated zone

3   of Yucca Mountain. Observed spatial distribution of fractures with coatings is used to

4   estimate the portion of active fractures. For a given survey interval along the tunnel, a

5   frequency of coated fractures can be estimated for a geologic unit based on the total

6   number of coated fractures. The ratio of the coated fracture frequency to the total fracture

7   frequency provides an estimate of portion of the active fracture for the given geologic

8   unit. The estimated average portion of active fractures for the TSw is about 7.2 %. Note

9   that fracture coatings may not precisely represent all the active flow paths in the

10   unsaturated zone of Yucca Mountain (Liu et al., 1998). Nevertheless, these values give

11   us at least an order-of-magnitude estimate of the portion of active fractures that is about

12   10 %.

13

14   Mineral-coating growth rate data imply that the unsaturated zone fracture network has

15   maintained a large degree of hydrologic stability over time, and that fracture flow paths

16   in the deep unsaturated zone are buffered from climate-induced variations in precipitation

17   and infiltration (Fabryka-Martin et al. 2000). If the AFM accurately represents water flow

18   processes, modeling results based on the AFM should be consistent with this important

19   observation.

20

21   **Comparison between Simulation Results and Field Observations**

22   One-dimensional dual-permeability numerical models are developed for boreholes

23   USW SD-12 and USW UZ-1. Calibrated rock properties (Liu and Ahlers, 2003) are used,

1   except for γ values associated with the TSw formation, where the repository is proposed

2   to be located. The value of the AFM parameter γ for the TSw formation is varied for

3   different simulations to check the sensitivity of simulated water travel times to this

4   parameter within the formation. The top boundary condition corresponds to the present-

5   day infiltration rate for flow simulations and a constant tracer concentration for transport

6   simulations. The initial condition for solute transport is zero concentration within the

7   fractured rocks. Previous studies indicate that dispersion processes have an insignificant

8   effect on overall solute transport behavior in unsaturated fractured rocks (Bodvarsson et

9   al., 2000; Liu et al., 2003b), and therefore are ignored here. An effective-diffusion-

10 coefficient value of 1.97E-10 m^2/s is employed, which is equal to the average value of

11 coefficients for tritiated water measured from tuff matrix samples. TOUGH2 and T2R3D

12 codes (Pruess, 1991; Wu et al., 1996) are used for simulating steady-state water flow and

13 tracer transport processes. Liu et al. (2000) reported good agreement between simulation

14 results using the above two codes for solute transport in the unsaturated zone of Yucca

15 Mountain and those obtained using a particle tracking method without numerical

16 dispersion, indicating that the effects of numerical dispersion are insignificant for the

17 problem under consideration. Simulated water travel times (or ages) for rock matrix are

18 compared with carbon-14 ages. A simulated water travel time at a location is determined

19 as the time when the matrix concentration reaches 50% of the top-boundary

20 concentration. It represents the average travel time for water particles from the ground

21 surface to the location under consideration.

22   Fig. 3 shows simulated water travel times (ages) for different γ values of the TSw

23 formation.   Note that a major path for tracer transport into the tuff matrix is from

1   fractures to the tuff matrix, which is different from tracer transport processes within a

2   single continuum. The considerable sensitivity of simulated results to γ indicates that

3   carbon-14 data are useful for validating the AFM and for constraining the γ values for the

4   TSw unit. For γ values ranging from 0.2 to 0.4, simulated results approximately match

5   the observations for the two boreholes simultaneously, although a better match is

6   obtained for USW SD-12 than that for USW UZ-14 (as a result of subsurface

7   heterogeneity). In our current model, the heterogeneity within each geological layer is not

8   considered. A larger γ value generally corresponds to a larger travel time (for the matrix),

9   because of the smaller degree of matrix diffusion resulting from a smaller fracture-matrix

10   interfacial area available for mass transport between fractures and the matrix (Eq. [10]).

11   Note that the observed carbon-14 ages and simulated water travel times result from a

12   combination of solute transport in fractures and the relatively slow matrix diffusion

13   process. The spatial variability of the degree of matrix diffusion is the reason why the

14   simulated water travel times and the observed ages in Fig. 3 are not always

15   monotonically increasing with depth in the TSw.

16

17   A sharp change in simulated water travel times occurs at an elevation of about 1,100 m

18   for two boreholes (Fig. 3). This is because the upper portion of the TSw unit has

19   relatively small fracture density values and therefore corresponds to a smaller degree of

20   matrix diffusion for a given γ value. For the borehole USW UZ-1, simulated water travel

21   time is generally longer than the observation for a given elevation. This may be owing to

22   a subsurface heterogeneity that gives larger fracture densities (resulting in a larger degree

23   of matrix diffusion) at the borehole location than what are used in the numerical model.

1   Layer-averaged fracture properties are used in the site-scale model of the unsaturated

2   zone of Yucca Mountain. In general, a comparison between simulated water travel times

3   and observed carbon-14 ages indicates that the AFM with γ values for the TSw between

4   0.2 to 0.4 can reasonably represent the data.

5

6   To check the consistency of the AFM with the coating data, a one-dimensional model

7   for borehole USW SD-12 is used. The model is the same as that described above. USW

8   SD-12 is chosen because it is located near the middle of the underground tunnel where

9   coating data were collected. Two infiltration rates (Flint et al., 1996), present day mean

10   infiltration rate (3.4 mm/yr) and glacial maximum infiltration rate (17.3 mm/yr), are used

11   for simulations. Again, uniform γ distributions for the TSw formation are employed. The

12   latter infiltration rate is about five times as large as the former rate and represents the

13   maximum infiltration rate in past climates.

14

15   Fig. 4 shows the simulated average portion of active fractures, f_a, for the TSw

16   formation as a function of infiltration rate and γ. The average portion is calculated from

17   Eq. [1] using the average effective saturation for the TSw formation. The calculated f_a

18   values are about 10 % to 40% for γ values ranging from 0.4 to 0.2 that are similar to those

19   used for matching the carbon-14 data. Recall that the estimate of the active fracture

20   portion from fracture coating data in the TSw was about 10%. Note that not all the active

21   flow paths are associated with coatings and that coatings can also disappear due to

22   dissolution. For example, Wang et al. (1999) found a flow feature under ambient

23   conditions from the unsaturated zone of Yucca Mountain. This flow feature does not have

coatings. Therefore, coated fractures may represent the lower limit of the number of active fractures at the Yucca Mountain site. Since the number of active fractures increases with γ, $\gamma = 0.4$ may roughly represent the upper limit for the actual γ values. For γ values less than 0.4, the calculated f_a values do not change significantly for the two infiltration rates (Figure 4), which is consistent with the observation of the stability of flow paths over time.

In summary, we have shown in this section that the AFM-based simulation results for $\gamma = 0.2 - 0.4$ approximately match the observed carbon-14 age data for the two borehole simultaneously. The similar range of γ value results in f_a values (for TSw) ranging from 10% to 40%, consistent with the portion of active fracture (10%) estimated from the fracture coating data. This portion (10%) is believed to represent the lower limit for f_a, as previously discussed. The insensitivity of f_a values for $\gamma = 0.2 - 0.4$ to infiltration rates is also consistent with the stability of flow paths over time that were observed from the unsaturated zone of Yucca Mountain. All these support the validity of the AFM.

CONCLUDING REMARKS

Accurately modeling flow and transport processes in natural unsaturated systems is very difficult, largely because these processes are generally localized and associated with fingering and preferential flow paths. While the continuum approach is still the most feasible choice for many large-scale problems encountered in the real world, the traditional continuum approach has generally failed in capturing localized flow behavior, because of the use of volume averaging at a subgrid scale.

1

2   Two schools of thought exist regarding how to address the problem mentioned above.

3   A number of researchers suggest using modeling approaches that are completely different

4   from the continuum approach, such as the DLA and percolation-based approaches (e.g.,

5   Ewing and Berkowitz. 2001; Glass 1993; Flury and Flühler 1995). These approaches

6   have been successfully used to represent relatively small-scale observations. However,

7   the use of these discrete approaches is very limited for large-scale applications.

8   Furthermore, completely satisfactory theories underlying these approaches are still

9   missing, and some critical steps in these approaches are somewhat arbitrary (Meakin and

10   Tolman, 1989; Ewing and Berkowitz, 2001).

11

12   The other school of thought is to modify the continuum approach by incorporating

13   key features of the discrete approaches (or small-scale observations), considering that the

14   continuum approach is computationally efficient and robust, and often preferred for

15   large-scale problems. Obviously, the AFM is a product of this school of thought. Note

16   that although these discrete approaches have different physical origins, they are

17   connected by the same class of flow patterns: fractals. Fractal flow behavior is also

18   supported by field observations from different unsaturated systems, including the

19   unsaturated zone of Yucca Mountain. Because of the relative simplicity of fractal-based

20   characterizations, we believe that the key small-scale features in unsaturated systems can

21   be successfully incorporated into large-scale continuum approaches. This is partially

22   supported by the consistency between simulation results based on the AFM and a variety

23   of field observations from the unsaturated zone of Yucca Mountain.

1

While we have demonstrated that the AFM is, in general, consistent with fractal flow behavior and can capture the major flow and transport features in the unsaturated zone of Yucca Mountain, more studies are needed to further improve it. For example, the AFM assumes a homogeneous distribution of flow field within the active-fracture continuum, whereas in reality the flow field may be very heterogeneous. One way to resolve this issue may be based on the concept of the multifractal (e.g., Feder 1988; Liu and Molz 1997). Another issue is that film flow is not explicitly considered in the current version of the AFM, while the film flow may be a potentially important mechanism of unsaturated flow in fractured rocks (Tokunaga and Wan, 1997). Note that the practical significance of film flow in unsaturated fractured rocks is still an issue of current debate (Tokunaga and Wan, 1997; Liu et al., 1998; Pruess et al., 1999; Or and Tuller, 2000; National Research Council, 2001). Field tests in the unsaturated zone of Yucca Mountain are also being currently performed with a major objective to further evaluate and improve the AFM. In the future, we will report on further evaluation of the AFM with data observed from these tests.

1

10

11

12

13

14

15

16

17

18

19

20

21

22

23

24

25

26

27

28

29

30

31

33

References

Bandurraga, T.M., and G.S. Bordvarsson. 1999. Calibrating hydrogeologic parameters for the 3-D site-scale unsaturated zone model of Yucca Mountain, Nevada. J. Contam. Hydrol. 38:47-46.

Bear, J., Tsang, C.F., de Marsily, G. (eds.). 1993. Flow and Contaminant Transport in Fractured Rock. Academic Press, San Diego, California.

Bodvarsson, G. S., and Y. Tsang, (Guest Editors). 1999. Yucca Mountain Project, *J.* Contam. Hydrol. 38:1-146.

Bodvarsson, G.S., H.H. Liu, R. Ahlers, Y.S. Wu and E. Sonnethal. 2000. Parameterization and upscaling in modeling flow and transport at Yucca Mountain, in Conceptual Models of Unsaturated Flow in Fractured Rocks, National Academy Press, Washington, D.C..

Brooks, R. H., and Corey, A.T. 1964. Hydraulic properties of porous media. Hydrol. Pap. No. 3. Colorado State Univ., Fort Collins.

Buscheck T.A., N.D. Rosenberg, J. Gansemer and Y. Sun. 2002. Thermohydrologic behavior at an underground nuclear waste repository. Water Resour. Res. 10.1029/2000WR00010.

Doughty, C. 1999. Investigation of conceptual and numerical approaches for evaluating moisture, gas, chemical and heat transport in fractured rock. J. Contam. Hydrol. 38: 69-106.

Ewing, R. P. and B. Berkowitz. 2001. Stochastic pore-scale growth models of DNAPL migration in porous media. Advances in Water Resources 24:309-323.

Fabryka-Martin J., A. Meijer, B. Marshall, L. Neymark, J. Paces, J. Whelan and A. Yang. 2000. Analysis of geochemical data for the unsaturated zone. Rep. ANL-NBS-HS-000017. CRWMS M&O, Las Vegas, Nevada.

Feder J. 1988. Fractals. Plenum Press, New York.

Flint, A.L., L.E. Flint, G.S. Bodvarsson, E.M. Kwicklis and J. Fabryka-Martin. 2001. Development of the conceptual model of unsaturated zone hydrology at Yucca Mountain, Nevada. in Conceptual Models of Unsaturated Flow in Fractured Rocks, National Academy Press, Washington, D.C.

Flint, A.L., J. A. Hevesi, E.L. Flint. 1996. Conceptual and numerical model of infiltration for the Yucca Mountain area, Nevada, Water Resources Investigation Report-96. U.S. Geologic Survey, Denver, Co.

Flury M. and H. Flühler. 1995. Modeling solute leaching in soils by diffusion-limited aggregation: Basic concepts and applications to conservative solutes. Water Resour. Res. 31; 2443-2452.

Gerke, H.H. and M. Th. Van Genuchten, 1993. A dual-porosity model for simulating the preferential movement of water and solutes in structured porous media. Water Resour. Res. 29: 305-319.

Glass R.J. 1993. Modeling Gravity-Driven fingering using modified percolation theory. In Proceedings of the fourth annual international conference on high level radioactive waste conference, Las Vegas, Nevada.

Glass, R. J., M. J., Nicholl, and V. C., Tidwell. 1996. Challenging and improving conceptual models for isothermal flow in unsaturated, fractured rocks through exploration of small-scale processes. Rep. SAND95-1824, Sandia National Laboratories, Albuquerque, NM.

Ho, C.K., 1997. Models of fracture-matrix interactions during multiphase heat and mass flow in unsaturated fractured porous media. Sixth symposium on multiphase transport in porous media, ASME International Mechanical Engineering Congress and Exposition, Dallas, TX.

Karasaki, K., S., Segan, K., Pruess, and S., Vomvoris. 1993. A study of two-phase flow in fracture networks. in Proceedings of the Fifth Annual International High-Level Radioactive Waste Management Conference, Am. Nucl. Soc., La Grange, IL.

Kwicklis, E. M., and R.W. Healey. 1993. Numerical investigation of steady liquid water flow in a variably saturated fracture network. Water Resour. Res., 29: 4091–4102.

Liu, H. H. and F.J. Molz. 1997. Multifractal analyses of hydraulic conductivity distribution. Water Resour. Res. 33: 2483-2488.

Liu, H. H., C. Doughty, and G. S. Bodvarsson. 1998. An active fracture model for unsaturated flow and transport in fractured rocks. Water Resour. Res. 34: 2633–2646.

Liu, H. H., G. S. Bodvarsson, and L. Pan. 2000. Determination of particle transfer in random walk particle methods for fractured porous media. Water Resour. Res. 36: 707-713.

Liu, H. H., and G. S. Bodvarsson. 2001. Constitutive relations for unsaturated flow in fracture networks. J. of Hydrology. 252: 116-125.

Liu, H.H., G.S. Bodvarsson and S. Finsterle. 2003a. A Note on unsaturated flow in two-dimensional fracture networks. Water Resour. Res. 38 (9), 1176, doi:10.1029/2001WR000977.

Liu, H.H., C. B. Haukwa, F. Ahlers, G. S. Bodvarsson, A. L. Flint, and W. B. Guertal. 2003b. Modeling flow and transport in unsaturated fractured rocks: An evaluation of the continuum approach. J. Contam. Hydrol. (in press).

Liu, H.H. 2000. Conceptual and numerical models for UZ flow and transport. Rep. MDL-NBS-HS-000005, CRWMS M&O, Las Vegas, Nevada.

Liu, H.H., and C.F. Ahlers. 2003. Calibrated properties model. Rep. MDL-NBS-HS-000003. BSC, Las Vegas, Nevada.

Mandelbrot B. B. 1982. The fractal geometry of nature. W.H. Freeman, New York.

Meakin P. and S. Tolman. 1989. Diffusion-limited aggregation. In Fractals in the natural sciences. Princeton Univ. Press, Princeton, N.J.

Molz, F.J., and G.K. Boman. 1993. A stochastic interpolation scheme in subsurface hydrology. Water Resour. Res. 29 :3769-3774.

Molz, F.J., H.H. Liu, and J. Szulga. 1997. Fractional Brownian motion and fractional Gaussian noise in subsurface hydrology: A review, presentation of fundamental properties, and extensions. Water Resour. Res. 33 : 2273-2286.

Moridis G. and Q. Hu. 2000. Radionuclide transport model under ambient conditions. Rep. MNL-NBS-HS-000008, CRWMS M&O, Las Vegas, Nevada.

Montazer P. and W.E. Wilson. 1984. Conceptual hydrologic model of flow in unsaturated zone, Yucca Mountain, Nevada. Water-Resources Investigation Report 84-4345. US Geologic Survey, Lakewood, CO.

National Research Council. 1996. Rock Fractures and Fluid Flow: Contemporary Understanding and Applications. National Academy Press, Washington, D.C.

National Research Council. 2001. Conceptual Models of Unsaturated Flow in Fractured Rocks, National Academy Press, Washington, D.C..

Neuman, S.P. 1990. Uinversal scaling of hydraulic conductivities and dispersivities in geologic media. Water Resour. Res. 26: 1749-1758.

Neuman, S.P. 1994. Generalized scaling of permeabilities: Validation and effect of support scale. Geophys. Res. Lett. 21:349-352.

Or, D., and M. Tuller 2000. Flow in unsaturated fractured porous media: Hydraulic conductivity of rough surfaces. Water Resour. Res. 36:1165-1171.

Perfect, E., N.B. McLaughlin, B.D. Kay, and G.C. Topp. 1996. An improved fractal equation for the soil water retention curve. Water Resour. Res. 32: 281-287.

Paces, J. B., L.A. Newmark, B.D. Marshall, J.F. Whelan, and Z.E. Peterman. 1996. Ages and origins of subsurface secondary minerals in the Exploratory Studies Facility. Milestone Rep. 3GQH450M. U. S. Geol. Surv., Denver, Colo.

Persson M., H. Yasuda, J. Albergel, R. Berndtsson, P. Zante, S. Nasri, and P. Ohrstrom. 2001. Modeling plot scale dye penetration by a diffusion limited aggregation (DLA) model. J. Hydrol. 250: 98-105.

Pruess, K. 1991. TOUGH2-A general purpose numerical simulator for multiphase fluid and heat flow. Rep. LBNL-29400. Lawrence Berkeley National Laboratory, Berkeley, CA.

Pruess, K., 1999. A mechanistic model for water seepage through thick unsaturated zones in fractured rocks of low matrix permeability. Water Resour. Res. 35: 1039-1051.

Pruess, K., B. Faybishenko, and G.S. Bodvarsson. 1999. Alternative concepts and approaches for modeling flow and transport in thick unsaturated zones of fractured rocks. J. Contam. Hydrol., 38: 281–322.

Rasmussen, T.C. 1991. Steady fluid and travel times in partially stractured fractures using a discrete air-water interface. Water Resour. Res. 27: 67-76.

Rieu, M., and G. Sposito. 1991a. Fractal fragmentation, soil porosity, and soil water properties, 1. Theory. Soil Sci. Soc. Am. J., 55:1231-1238.

Rieu, M., and G. Sposito. 1991b. Fractal fragmentation, soil porosity, and soil water properties, 2. Applications. Soil Sci. Soc. Am. J., 55: 1231-1238.

Robinson, B.A., A.V. Wolfsberg, H.S. Viswanathan, G. Bussod, C.W. Gable, and A. Meijer. 1997. The site-scale unsaturated zone transport model of Yucca Mountain. LANL milestone report SP25BMD.

Smith J.E. and Z. F. Zhang. 2001. Determining effective interfacial tension and predicting finger spacing for DNAPL penetration into water-saturated porous media. J. Contam. Hydrol. 48: 167-183.

Stauffer D. and Aharony, A. 1991. Introduction to Percolation Theory. Tayler & Francis.

Su, G.W., J.T. Geller, K. Pruess, and F. Wen. 1999. Experimental studies of water seepage and intermittent flow in unsaturated rough-walled fractures. Water Resour. Res., 35: 1019-1037.

Van Genuchten, M. 1980. A closed-form equation for predicting the hydraulic conductivity of unsaturated soil. Soil Sci. Soc. Amer. J. 44: 892-898.

Tokunaga, T. K., and J. Wan. 1997. Water film flow along fracture surface of porous rock. Water Resour. Res. *33*: 1287-1295.

Tyler, S.W., and S.W. Wheatcraft. 1990. Fractal processes in soil water retention. Water Resour. Res. 26:1047-1054.

Wang J.S.Y., R.C. Trautz, P.J. Cook, S. Finsterle, A.L. James and J. Birkholzer. 1999. Field tests and model analyses of seepage into drift. J. Contam. Hydrol. 38:232-347.

Wang Z., Feyen J., and Elrick D.E. 1998. Prediction of fingering in porous media. Water Resources Research 34:2183-2190.

Witten, T.A. and L. M. Sander. Diffusion-limited aggregation: A kinetic critical phenomenon. Phys. Rev. Lett. 47: 1400-1403.

Wilkinson D. and J.F. Willewsen. 1983. Invasion percolation: A new form of percolation theory. J. Phys. A. 16:3365-3376.

Wu Y. S., L. Pan, W. Zhang and G.S. Bodvarsson. 2002. Characterization of flow and transport processes within the unsaturated zone of Yucca Mountain, Nevada, under current and future climates. J. of Hydrology. 54: 215-247.

Wu, Y.S., J. Liu, T. Xu, C. Haukwa, W. Zhang, H.H. Liu, C.F. Ahlers. 2000. UZ flow models and submodels. Rep. MDL-NBS-HS-000006, CRWMS M&O, Las Vegas, Nevada.

Wu, Y. S., C.F. Ahlers, P. Fraser, A. Simmons, K. Pruess, 1996. Software qualification of selected TOUGH2 modules. LBNL-39490, Lawrence Berkeley National Laboratory, Berkeley, CA.

Xu T., E. Sonnenthal, and G. S. Bodvarsson. 2003. A reaction-transport model for calcite precipitation and evaluation of infiltration fluxes in unsaturated fractured rock. J. Contam. Hydrol. (in press).

Yamamoto H., K. Kojima and H. Tosaka, 1993. Fractal clustering of rock fractures and its modeling using cascade process. In Scale Effects in Rock Masses 93, Pinto da Cunha (ed.). 1993 Balkema, Rotterdam.

Yang, I.C. 2002. Percolation flux and transport velocity in the unsaturated zone, Yucca Mountain, Nevada. Applied Geochemistry. 17: 807-817.

Zhou Q., H.H. Liu, G.S. Bodvarsson, and C. M. Oldenburg. 2003. Flow and transport in unsaturated fractured rock: Effects of multiscale heterogeneity of hydrogeologic properties. J. Contam. Hydrol. 60: 1-30.

Zimmerman, R.W., and G.S. Bodvarsson. 1996. Effective transmissivity of two-dimensional fracture networks. Int. J. Rock Mech. Min. Sci. 33: 433-438.

(a) l = L

(b) l = L/2

(c) l = L/4

(d) l = L/8
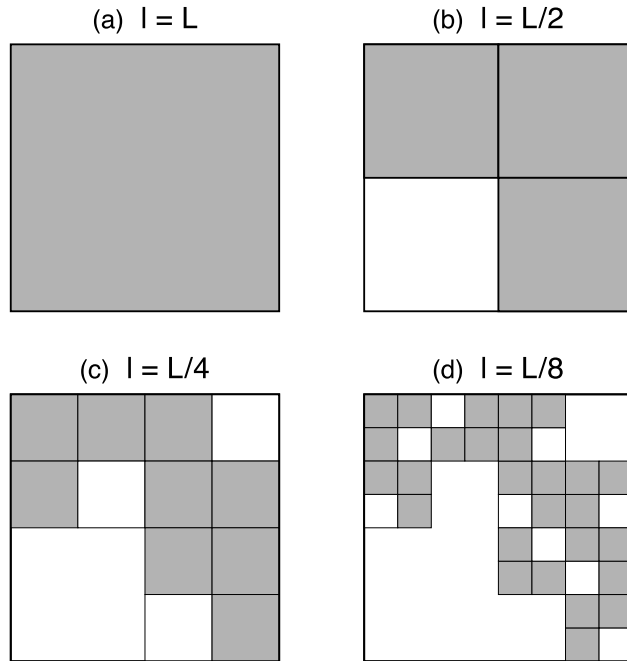
AT03-002

Fig. 1. Demonstration of the "box" counting procedure for several box sizes
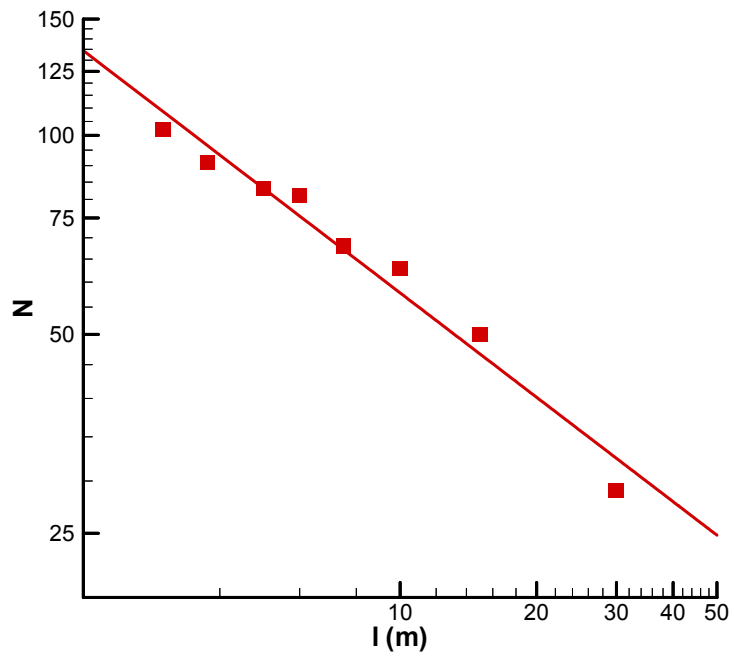
Fig. 2. Relation between the number of box (N), covering at least one intersection between coated fractures and the survey line, as a function of box size l. The solid line corresponds to a power function (with a power of – 0.5) used to fit the data points.
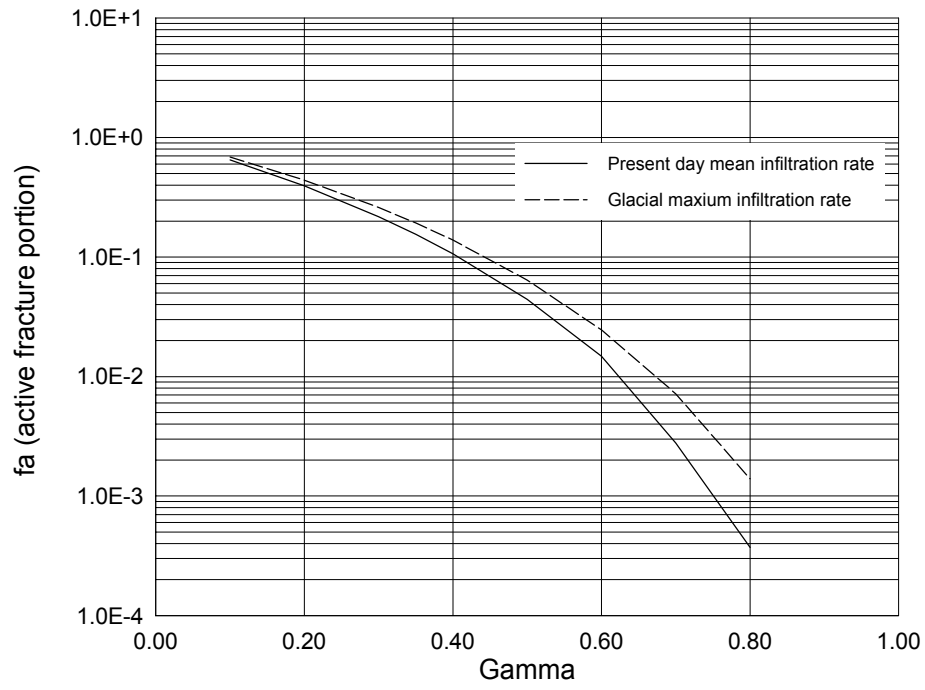
1
2   (a)

3
4   (b)
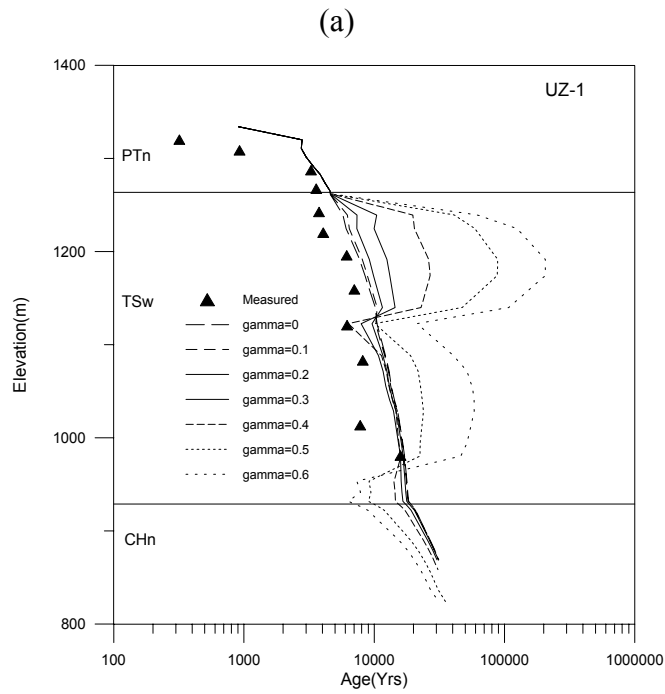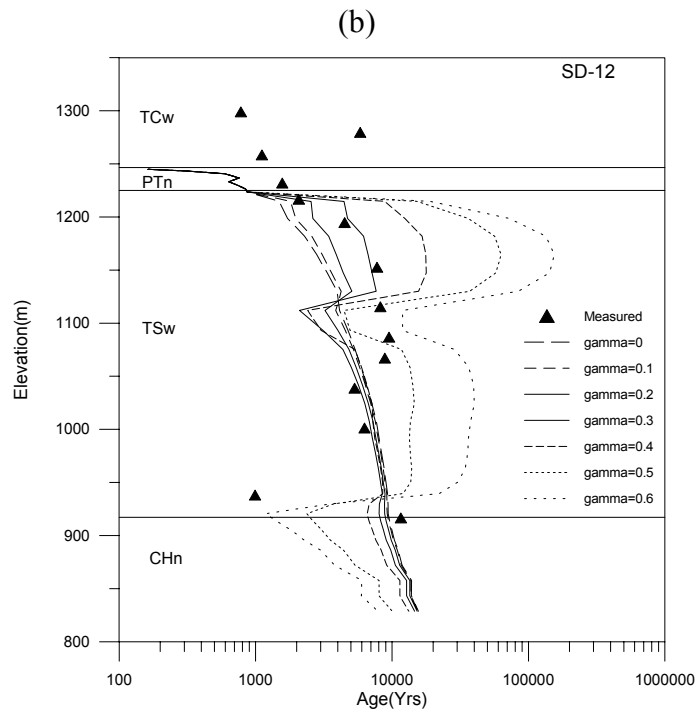
5
6   **Figure 3.** Comparisons between simulated water travel times (ages) for rock matrix at
7 boreholes (a) USW UZ-1 and (b) USW SD-12 and the corresponding Carbon-14 ages for several
8   γ values.
9

10
11

1

2
3
4   **Fig. 4**. Simulated average portion of active fracture for the TSw formation as a function
5   of infiltration rate and γ.
6
7
8
9